AFRL-RX-WP-TP-2011-4366

DEVELOPMENT OF A NONDESTRUCTIVE NON-CONTACT ACOUSTO-THERMAL EVALUATION TECHNIQUE FOR DAMAGE DETECTION IN MATERIALS (PREPRINT)

J.T. Welter and K.V. Jata

Nondestructive Evaluation Branch (AFRL/RXLP)

S. Sathish, N. Schehl, and T.R. Boehnlein

University of Dayton

NOVEMBER 2011

AIR FORCE RESEARCH LABORATORY
MATERIALS AND MANUFACTURING DIRECTORATE
WRIGHT-PATTERSON AIR FORCE BASE, OH 45433-7750
AIR FORCE MATERIEL COMMAND
UNITED STATES AIR FORCE

REPORT DOCUMENTATION PAGE

Form Approved
OMB No. 0704-0188

1. REPORT DATE *(DD-MM-YY)*	2. REPORT TYPE	3. DATES COVERED *(From - To)*
November 2011	Technical Paper	1 November 2011 – 1 November 2011

4. TITLE AND SUBTITLE
DEVELOPMENT OF A NONDESTRUCTIVE NON-CONTACT ACOUSTO-THERMAL EVALUATION TECHNIQUE FOR DAMAGE DETECTION IN MATERIALS (PREPRINT)

5a. CONTRACT NUMBER
FA8650-09-D-5224

5b. GRANT NUMBER

5c. PROGRAM ELEMENT NUMBER
62102F

6. AUTHOR(S)
J.T. Welter and K.V. Jata (AFRL/RXLP)
S. Sathish, N. Schehl, and T.R. Boehnlein (University of Dayton)

5d. PROJECT NUMBER
4349

5e. TASK NUMBER
40

5f. WORK UNIT NUMBER
LP102200

7. PERFORMING ORGANIZATION NAME(S) AND ADDRESS(ES)
University of Dayton
300 College Park Avenue
Dayton, OH 45469

8. PERFORMING ORGANIZATION REPORT NUMBER

9. SPONSORING/MONITORING AGENCY NAME(S) AND ADDRESS(ES)
Air Force Research Laboratory
Materials and Manufacturing Directorate
Wright-Patterson Air Force Base, OH 45433-7750
Air Force Materiel Command
United States Air Force

10. SPONSORING/MONITORING AGENCY ACRONYM(S)
AFRL/RXLP

11. SPONSORING/MONITORING AGENCY REPORT NUMBER(S)
AFRL-RX-WP-TP-2011-4366

12. DISTRIBUTION/AVAILABILITY STATEMENT
Approved for public release; distribution unlimited.

13. SUPPLEMENTARY NOTES
This work was funded in whole or in part by Department of the Air Force contract FA8650-09-D-5224. The U.S. Government has for itself and others acting on its behalf an unlimited, paid-up, nonexclusive, irrevocable worldwide license to use, modify, reproduce, release, perform, display, or disclose the work by or on behalf of the U.S. Government. PA Case Number and clearance date: 88ABW-2011-3946, 19 Jul 2011. Preprint journal article to be submitted to Review of Scientific Instruments. This document contains color.

14. ABSTRACT
This paper presents the development of a new non-contact acousto-thermal signature (NCATS) nondestructive evaluation (NDE) technique. The physical basis of the method is the measurement of the efficiency of the material to convert acoustic energy into heat, and a theoretical model has been developed. The increase in temperature due to conversion of acoustic energy injected into the material without direct contact was found to depend on the thermal and elastic properties of the material. In addition, it depends on the experimental parameters of the acoustic source power, the distance between sample and acoustic source, and the period of acoustic excitation. Systematic experimental approaches to optimize each of the experimental variables to maximize the observed temperature changes are described. The potential of the NCATS technique to detect microstructural-level changes in materials is demonstrated by evaluating accumulated damage due to plasticity in Ti-6Al-4V and low level thermal damage in polymer matrix composites.

15. SUBJECT TERMS
hysteretic heating, polyimide resin, nondestructive evaluation

16. SECURITY CLASSIFICATION OF:			17. LIMITATION OF ABSTRACT:	18. NUMBER OF PAGES	19a. NAME OF RESPONSIBLE PERSON (Monitor)
a. REPORT	b. ABSTRACT	c. THIS PAGE			John Welter
Unclassified	Unclassified	Unclassified	SAR	34	19b. TELEPHONE NUMBER *(Include Area Code)* N/A

Development of Nondestructive Non-Contact Acousto-Thermal Evaluation Technique for Damage Detection in Materials

Shamachary Sathish[*], John T Welter, Kumar V Jata, Norman Schehl[*], Thomas Boehnlein[*]

Metals, Ceramics and Nondestructive Evaluation Division

Air Force Research Laboratory, Wright-Patterson Air Force Base, Dayton, OH

[*]Structural Integrity Division

University of Dayton Research Institute

300 College Park, Dayton, OH

ABSTRACT

This paper presents the development of a new non-contact acousto-thermal signature (NCATS) nondestructive evaluation (NDE) technique. The physical basis of the method is the measurement of the efficiency of the material to convert acoustic energy into heat, and a theoretical model has been developed. The increase in temperature due to conversion of acoustic energy injected into the material without direct contact was found to depend on the thermal and elastic properties of the material. In addition, it depends on the experimental parameters of the acoustic source power, the distance between sample and acoustic source, and the period of acoustic excitation. Systematic experimental approaches to optimize each of the experimental variables to maximize the observed temperature changes are described. The potential of the NCATS technique to detect microstructural-level changes in materials is demonstrated by evaluating accumulated damage due to plasticity in Ti-6Al-4V and low level thermal damage in polymer matrix composites. The ability of the technique for macroscopic applications in nondestructive evaluation is demonstrated by imaging a crack in an aluminum test sample.

INTRODUCTION

Mechanical loading of materials is well known to cause temperature changes [1-3]. Inducing temperature changes in materials, components, and structures through mechanical loading and capturing the temperature change using a sensitive infrared (IR) camera has been used effectively for nondestructive evaluation [4-7]. In general such methods have been given different names such as vibrothermography, thermosonics, and Sonic IR. [8-10]. The method has been effective in the detection of defects such as cracks and delaminations in metallic, ceramic, and polymer matrix composites. One of the major advantages of this technique is that large structures and structures with complex curvature can be evaluated. The source of the thermal gradient in the temperature images that identifies these types of defects has been attributed to the rubbing of the closed faces of a crack or delamination [11, 12].

Experimentally, a small difference between vibrothermography [4, 9, 10] and thermosonics/Sonic IR [8, 11, 12] can be recognized. In vibrothermography, the structure is physically attached to a mechanical excitation source, such as a dynamic shaker or vibrator, operating at frequencies from a few Hz to several kHz. In thermosonics an ultrasonic horn, of the type often used for plastic welding, is used where the structure or component is physically contacted by the ultrasonic horn and is excited at tens of kHz. A problem with the contact based thermosonic method is in producing a consistent contact between the horn and the sample to obtain a repeatable excitation for detection of the damage of interest. Varieties of materials, including card stock, leather, Teflon, aluminum sheet and foil, and copper, have been used to produce a repeatable contact with some degree of success [13]. The location of test sample clamping points, pressure applied at the clamps, and pressure applied at the horn tip have been reported to affect results as well. Another problem is the high energy and high amplitudes at which the horn is operated. In contact with sample the horn in effect hammers the sample [14]. It has been suggested that contact excitation of this type will induce damage in the sample if not applied correctly. This is supported by literature illustrating the use of a 20 kHz ultrasonic horn to produce high cycle fatigue in samples [15-17]. However, proper

management of the coupling process and excitation parameters can be used to mitigate this risk.

In general, studies are reported in the literature [4-19] concerning mechanical excitation of materials through physical contact and observation of heat generation that have established the basic principles of acousto-thermal based nondestructive evaluation (NDE) methodology for defect and damage evaluation. A major challenge to the adoption of an acousto-thermal based technique for NDE is the requirement to dynamically load the specimen/component. Designs of fixtures for components and specimens to resonate at appropriate acoustic frequency are very challenging. Thus the technique has remained a laboratory tool for evaluation of materials. The basic principle of the technique presented here is the excitation of a material with high amplitude acoustic waves without contact between the specimen and excitation source, and measuring the change in the temperature caused by the interaction of acoustic waves with the material. When the material undergoes a change that alters the acousto-thermal coupling, the interaction between the acoustic waves and the material is modified, causing a change in the expected temperature distribution in the material due to the acoustic excitation. The basic mechanism of interaction between material and ultrasonic wave to generate heat is described in Section I. The experimental setup is described in Section II. Optimization and calibration of individual components of the instrument to observe non-contact acousto-thermal signatures in the material is described in Section III. To illustrate the applications of the non-contact acousto-thermal technique, three examples are presented in Section IV. The examples investigate accumulation of plasticity in Ti-6Al-4V, detection of incipient thermal damage in polymer matrix composite plate, and detection and imaging of a crack in an aluminum alloy component.

I. Heat generation due to acoustic wave interaction with the material

When acoustic waves propagate in a material, part of the energy is lost to the material due to absorption and scattering, a portion is reflected back to the source by the material, and the remaining part is transmitted through the material. Part of the absorbed energy is converted to heat, which is known as thermo-elastic loss. The temperature changes due to

a thermo-elastic loss can be evaluated by analyzing the acoustic wave propagation in materials [20, 21]. Consider a sinusoidal acoustic wave,

$$\sigma = \sigma_o \sin \omega t \quad (1),$$

propagating in the material where σ is the stress at any time t, σ_o is the maximum amplitude, $\omega = 2\pi f$, and f is the frequency of the acoustic wave. This produces a sinusoidal strain ε, in the material which will be out of phase with the stress by a phase angle δ. Following Nowick and Berry [22], the average energy dissipation per cycle is,

$$W = 2\pi \ \mathrm{Tan}\delta \left(\frac{\sigma_{max}^2}{2E} \right) \quad (2).$$

where Tan δ, is the internal friction in the material, E is the Young's modulus and σ_{max} is the maximum amplitude of the acoustic wave. Assuming that all the dissipated energy is converted into heat under adiabatic conditions, the rate of change of temperature per unit volume of the material is,

$$\frac{dT}{dt} = \frac{2\pi f \ \mathrm{Tan}\delta}{\rho C_p} \left(\frac{\sigma_{max}^2}{2E} \right) \quad (3)$$

where ρ is the density of the material and C_p is the specific heat at constant pressure.

Considering heat loss to the environment, the rate of change of temperature can be written as,

$$\frac{dT}{dt} = \frac{2\pi f \ \mathrm{Tan}\delta}{\rho C_p} \left(\frac{\sigma_{max}^2}{2E} \right) - \frac{k}{\rho C_p}(T - T_0) \quad (4)$$

where k is the thermal conductivity of the material and T_o is the ambient temperature. Equation (4) shows that the conversion of acoustic energy to thermal energy depends on both the elastic properties (E and tan δ) and the thermal properties (k, C_p) of the material. It is clear that a change in one or more material properties (k, C_p, E and Tan δ) will result

in a change in acousto-thermal energy conversion, and therefore a change in the amount of thermal energy observed. This is the basis of the acousto-thermal NDE technique described here.

II. Experimental method

A schematic of the experimental setup used for non-contact acousto-thermal signature (NCATS) measurement is provided in Figure 1. The instrumentation consists of a high amplitude acoustic wave generator (900 BCA, Branson Ultrasonics) operating at 20 kHz with a maximum power output of 1000W. A sample is placed just ahead of the tip of the horn, with an air gap between the horn and the sample. An infrared (IR) camera (Merlin Mid-IR, Indigo Inc.) is placed on the opposite side of the sample to image the temperature change in the sample. A computer is used to capture and analyze the temperature data. When the high amplitude acoustic generator is excited the acoustic waves propagate through the air gap and interact with the sample. Part of the acoustic wave energy is reflected off the front interface and, part is transmitted into the sample. A portion of the acoustic energy is transmitted through the sample, and a portion is absorbed by the sample. The absorbed energy is converted into heat. The heat generated increases the temperature of the sample and the IR camera detects the temperature changes.

Since the acoustic horn does not come into contact with the sample during acoustic excitation, the temperature change observed is only due to the conversion of acoustic energy into heat and depends on the amplitude of the acoustic wave incident on the sample, the distance between sample and the horn, and the material properties of the sample. The temperature change in the sample is typically only a few degrees and requires a high sensitivity camera for accurate detection. The measurements are performed at ambient temperature, and the sensitivity of the IR camera should be very high in the range of 20º to 25º C. Hence a careful calibration is required. From equation (4) it is clear that the temperature change in the sample depends on the amplitude of the acoustic waves interacting with the sample. The acoustic wave amplitude varies inversely with the distance from the acoustic horn. Therefore, a minimum distance between the

sample and the acoustic horn will yield the best signal to noise ratio. However, for non-contact acoustic interaction with the sample, the acoustic horn must not come into contact with the sample at any excitation power. This requires an accurate characterization of the acoustic horn displacements to determine the minimum distance between the sample and the acoustic horn.

a. Acoustic horn displacement and positioning

The high amplitude acoustic horn consists of a stack of piezo-electric transducers. When the stack is excited by a 20 kHz sinusoidal signal, the longitudinal elongations of each of the transducers in the stack add to produce a large longitudinal strain. This strain is amplified by a mechanical booster. The strain generated by the booster is further amplified by an exponential horn designed to produce its highest strain at the tip. The horn is designed to have a tip that is an anti-node and displaces like a piston. The piston like behavior of the horn tip was confirmed by measuring the out of plane displacement of the horn tip with a laser vibrometer (Polytec model PSV-400, OFV-5000). Although the motion was viewed in three dimensions as a movie, Figure 2 shows the view at two extreme positions of maximum and minimum displacements and the neutral position. It can be seen that the face of the horn moves like a piston when excited.

The acoustic horn displacement measurements were performed utilizing an optical fiber displacement sensor (Model D20+H1PQ, Philtec, Inc.) in front of the acoustic horn. The acoustic horn was excited with different power levels, and the wave form of the acoustic signal and the absolute acoustic displacement was measured and recorded. Figure 3 shows the absolute displacement of the horn tip for different excitation powers. The horn output is measured in terms of percent of the maximum power. In the range of power of 500W through 1000W, the acoustic displacement is linear and the maximum displacement was 180 μm at the highest power level (1000W). These measurements are used to determine the distance between the sample and the horn to ensure the horn does not contact the sample during acoustic excitation.

Characterization of the acoustic displacements of the horn, as a function of input power, determines the distance between the sample and the horn to prevent contact. The distance

between the horn and the sample was set using mechanical methods. For ease of operation the stack, the booster, and the exponential horn were assembled and set horizontally on a support. A manual translation stage with micrometer is attached to the support to enable and track the movement of the horn along its long axis. For mechanically adjusting the distance, the acoustic horn was moved using the micrometer to bring the acoustic horn into contact with the sample and establish the zero position. From this point the micrometer was used to back the horn off the desired distance to ensure it did not contact the sample when activated yet allowed maximum displacement. This method was quite simple, easy to use, and works with any material. A drawback of the method was that physical contact has to be determined by visual observation and operator experience. To remove operator bias when the sample is electrically conductive, an electrical resistance measurement can be used to determine contact. In this method, the sample and the acoustic horn form part of an electrical circuit and the circuit resistance was monitored to determine when contact occurs. When the two are not in contact the resistance will be greater than 1 MΩ and less than 100 Ω when contact exists. This method was reliably used to establish the physical contact between an electrically conductive sample and the horn. Once contact was established, the acoustic horn was set to the desired standoff distance using the micrometer.

Characterization of the temperature sensitivity of infrared camera

The changes in the temperature of the specimen due to acoustic excitation are imaged and measured with the IR camera. The manufacturer quoted noise equivalent temperature difference (NETD) is 0.025K. Although this was a measure of the high sensitivity of the IR camera, the minimum temperature that can be resolved by the camera depends on the A/D digitization rate and the temperature range in which the camera was used [23, 24]. In the NCATS experiments, the temperature changes due to acoustic excitation are in the range of 0.1 to 2 °C from ambient. Since the temperature changes are small, the camera sensitivity was examined between room temperature and 35 °C. A black target was immersed in a temperature controlled water bath (Haake DC30) and heated from 22°C to 35°C in steps of 0.5°C. The temperature of the black target was set to desired temperature with a resolution of +/- 0.01 °C using the temperature controller. The temperature of the

black target was measured with the IR camera. The sensitivity of the IR camera in the temperature range of 22º to 35º C was found to be linear and the sensitivity was determined as 0.0125 ºC per count.

Characterization of Acoustic Horn Temperature

In the non-contact acousto-thermal technique the interaction of acoustic energy with the sample is expected to produce a small change in the temperature. To ensure that the temperature being imaged is only due to conversion of acoustic energy to heat, other sources of heat needed to be eliminated. From the experimental setup it can be recognized that the acoustic horn was closer to the sample than any other component of the system. It is reasonable to assume that the large displacements of the horn would cause the horn to heat by similar thermo-elastic effects, and this heat might be conducted to the sample resulting in temperature changes in the sample. This was explored by imaging the acoustic horn tip with an IR camera at increasing amounts of input power (500W through 1000W) and periods of excitation from 250 ms to 1000 ms. The temperature of the tip of the acoustic horn did not change for any combination of input power levels and excitation duration tested. The length of the acoustic horn was designed to be equal to a quarter wavelength, with the tip being an anti-node for maximum longitudinal displacement. In a bar undergoing longitudinal resonances, the nodes are formed at maximum compression while the antinodes are at maximum elongation. The temperature at the nodes will be a maximum while at anti-nodes it will be a minimum. Thus, at the anti-node (tip) of the horn the temperature rise is expected to be a minimum. The tip of the horn is a free surface vibrating in air with minimum resistance while propagating acoustic waves into the air. The combination of the tip being an anti-node and the tip moving freely in air with minimum resistance appear to be reasons that there was no observable change in temperature at the horn tip during the excitation at all input power levels and durations tested.

Measurement of temperature changes in the sample due to acoustic excitation

The basic physical mechanism in the conversion of acoustic energy to heat in a sample is described in eq. (4), and it shows that the conversion depends on the frequency and

amplitude of acoustic excitation, absorption of acoustic energy, Young's modulus, specific heat, and thermal conductivity of the material. Apart from the intrinsic physical properties, to observe a measurable increase in temperature the experimental parameters need to be optimized. These parameters include, i) the input power to the acoustic horn, ii) duration of the acoustic horn excitation, and iii) distance between the sample and the horn tip. An experiment using a sample of Ti-6Al-4V was performed to investigate and optimize the experimental parameters.

a. Temperature changes in the sample for fixed distance between sample and the horn, fixed excitation time and varying input power.

The distance between the acoustic horn and the sample was set at 300 μm. The excitation time of the horn was fixed at 250 ms and the time-temperature response was measured at different power levels from 500 W to 1000 W in 100 W increments. Figure 4, shows the time-temperature response for six different input powers collected over a period of 2.75 s. It is clear from the figure that the temperature of the sample increased rapidly, attained a maximum and then decreased slowly. In general for all input powers, the shape of the curves is similar. The maximum temperature attained by the sample increased with increasing excitation power. The sample reached maximum temperature after 250 ms after acoustic excitation for all the input powers. It is interesting to note that the time-temperature behavior observed in NCATS measurements is similar to the laser flash method used to measure thermal properties of materials [25] and conventional thermography used in NDE technique [26, 27].

b. Temperature changes in the sample for fixed power and fixed distance for different excitation durations

The sample-horn distance was set to 200 μm, such that for a 1000 W excitation there is no contact between the sample and the acoustic horn. The time-temperature response was collected for excitation durations (pulse lengths) of 250ms, 500ms, 750ms and 1000ms and is shown in Figure 5. The general features of the time-temperature responses are similar to Figure 4. For all excitations the temperature of the sample increased to a maximum and then decreased gradually. The maximum temperature attained by the

sample increased with increasing acoustic excitation duration. The time required for the sample to reach maximum temperature increased with the duration of excitation from 685 ms for 250 ms excitation time to 1335 ms for 1000 ms excitation period

c. Temperature changes for fixed input power and fixed duration of excitation for varying distances between sample and the horn

To examine the temperature changes for fixed input power and fixed duration of excitation for varying distances between sample and the horn, the input power was held constant (1000 W or 800 W) and duration of excitation was chosen to be 250 ms. The distance between the horn and the sample was varied using the micrometer attached to the acoustic horn. Care was taken to set the distance such that the horn would not contact the sample, a minimum of 180 μm. At each distance time-temperature response was obtained and the maximum temperature attained by the sample was determined. Figure 6 shows the variation of maximum change in temperature with distance between the sample and the horn for excitation power of 1000W and 800W. The measurements show that the maximum temperature change in the sample decreases with increasing separation between the sample and the acoustic horn.

Analysis of measurement of change in temperature of the sample due acoustic interaction shows that it depends on the input power to the horn, distance between the sample and the horn and the duration of excitation. The change in the temperature of the sample increases with increasing input power, for a fixed distance between sample and the horn and duration of excitation of the horn. On the other hand it decreases with increased distance of separation between sample and the horn. The results of the measurements are used to optimize the temperature observed in a material by adjusting the input power to the horn, duration of excitation and distance between the sample and the horn.

Demonstration of the applicability of NCATS

Three different types of samples, flat dog bone Ti-6Al-4V, polymer matrix carbon fiber composites and aircraft aluminum alloy wheel were used to demonstrate the applicability of the NCATS system. Ti-6Al-4V samples were used for examining the optimization of the NCATS system and to evaluate damage due to plasticity. Polymer matrix composite samples were used to demonstrate the capability of the NCATS technique to evaluate incipient thermal damage in composite structures. An aluminum aircraft wheel with a crack was used to show the applicability of the technique for nondestructive evaluation and detection of defects (cracks) in components.

a. Accumulated damage due to tensile loading

It is well known that ductile metallic materials undergo plastic deformation under uniaxial loading beyond the yield stress. With continued loading the material will reach its ultimate stress and further loading will cause it to fracture. The relationship between the stress-strain curve and changes in microstructure during deformation in ductile metallic materials has been studied over the last several decades, and a general understanding has been obtained. In the elastic region, the material can recover with no measurable changes in behavior or structure. Beyond the yield stress, due to the generation, accumulation, and motion of dislocations, the metal can no longer completely recover from the induced strain. The accumulation of dislocations increases the hardness. Continued plastic deformation increases dislocation density until the beginning of necking and void formation. Voids form at favorable locations in the microstructure and grow in the interior of the sample with continued plastic deformation. Micro-cracks form later due to void coalescence or void growth. Eventually the micro-cracks grow large enough and cause the sample to fracture.

A ductile material subjected to stresses beyond the elastic limit contains accumulated damage in the form of increased dislocation and evolving dislocation structure. The accumulated damage can produce a small (of 0.1% to 1%) change in the elastic modulus, electrical conductivity and thermal conductivity. Thus, conventional NDE techniques based on ultrasonic, eddy current, and thermographic methods have limited ability to detect this relatively low level damage caused by plasticity. This is because conventional NDE techniques measure the elastic modulus, damping, thermal

conductivity or specific heat individually, and in many cases the measurement methods do not have the sensitivity to observe the very small changes in these parameters due to plasticity. NCATS does not measure a single property, but a combined effect. As evident in Equation (4), the NCATS signature is not only sensitive to the elastic modulus, thermal conductivity, and specific heat, but the internal friction (tan δ) has critical contribution to temperature changes. It is clear from equation(4), that the NCATS response is a combination of multiple physical properties and a small change in any one may lead to an observable change in ΔT, thus improving the detection of small material property changes in a material due to plasticity.

To demonstrate the feasibility, flat dog-bone Ti-6Al-4V samples having a gage section of 25.4mm x 12.7mm x 2.3mm were used in experiments. The material had an equiaxed microstructure comprised of 60% of primary alpha and 40% alpha-beta lamellas, an average grain size of 20 μm, and less than 10% crystallographic texture [28, 29]. The samples were annealed to remove any residual stresses resulting from machining. The removal of residual stress was confirmed by X-ray diffraction residual stress measurements.

The NCATS tests were performed with a stand-off distance of 200 μm between the sample and the ultrasonic horn, pulse duration of 1 s, and the horn power set at 1000 W. The pulse duration and power were the same for all the measurements. A servo-hydraulic test machine was used to plastically deform the sample, while the strain in the sample was measured with an extensometer. The sample was strained in increments of 2%, and the load was brought to zero after each strain increment for NCATS measurements. After each measurement the sample was subsequently loaded and the plastic strain was increased by 2%. This was continued until the sample fractured. A computer controlled data acquisition system was used to record the load, displacement, strain and temperature measurements during the experiments. From the change in temperature versus time (ΔT-t) data, the maximum change in the temperature (ΔT_{max}) realized by the sample during the acoustic excitation was determined. A composite stress-strain to fracture curve was also built from the stress-strain curve of each increment of plastic strain. The variation of ΔT_{max} with accumulated strain in the sample is shown in Figure 7. The composite stress-strain (σ–ε) curve is provided in Figure 8.

The NCATS temperature change measurement as a function of strain has a different behavior compared to the stress-strain curve. The temperature change is unchanged, 1.6 C until the strain increased beyond 4%. The temperature change increased approximately linearly up to 14% strain, reaching a maximum of plastic strain and beyond the temperature decreased with increasing strain until sample fractured at greater than 20% strain.

Although the temperature changes are sensitive to the plastic strain, the maximum did not occur at the ultimate strain in the sample. The ultimate stress occurred at a strain of 10-11%, the maximum change in temperature in the NCATS measurements occurred at 14% strain. One possible explanation for the increased contribution to heating is the formation of internal voids prior to the onset of ultimate stress and creation of micro-cracks due to growth or coalescence of voids. During acoustic excitation, opposing faces of the voids and cracks can rub against each other, producing additional frictional heating [30] that makes the temperature changes in the sample to appear at 14% strain rather than at 10-11% expected at the ultimate stress inferred from stress-strain curve. Beyond 14% of strain, the crack faces separate significantly and do not produce frictional heating during acoustic excitation. X-ray computer tomography of the fractured sample showed the presence of cracks with separation widths of 7-10 μm [30] that is much larger than the displacements that can be produced by the acoustic excitation in the sample.

b. Heat damage in polymer matrix composite

When exposed to temperatures approaching or exceeding the glass transition temperature, the strength of polymer matrix composites (PMCs) has been found to decrease. When the temperature is high enough the damage can be seen as charring, blistering and other obvious surface features. This is extensive damage that can be detected visually without much difficulty. When the damage is not visible, ultrasonic and thermography NDE techniques have been valuable in detecting damage due to sub-surface delamination. Thermal exposure of PMCs can cause subtle damage that may not induce delaminations. This low level “incipient damage” has been shown to decrease the strength significantly [31, 32]. During exposure to high temperatures, both physical and chemical properties of the polymer matrix can change, including properties such as elastic modulus, density,

thermal expansion, thermal conductivity, or heat capacity. The basic physical mechanisms of NCATS, as described by eq. (4) are sensitive to many of the thermal and elastic properties that change in polymers during thermal exposure. It is the combination of thermal properties, elastic properties and the density that yields the temperature change produced by NCATS. Therefore, NCATS should be sensitive to incipient thermal damage in polymer matrix composites.

Polymer matrix composite samples with carbon fibers in epoxy were used to demonstrate the sensitivity of NCATS to heat damage. A flat plate sample was exposed to high temperatures by focusing heat generated by a lamp onto a spot. Different regions on the sample were exposed to high temperature for different amounts of time while the lamp distance and focal spot area were kept constant. Three regions with exposure times of 180 s, 360 s and 540 s producing light, medium and heavy damage regions were chosen for measurements and compared with an undamaged region. NCATS measurements were performed by placing the region of the sample just ahead of the horn tip (distance of 200 μm). The time-temperature (ΔT-t) data was collected on the opposite side of the sample in line with the horn for varying input power to the horn (500W to 1000W). Maximum change in the temperature of the region on the sample was determined for each of the locations. Figure 9 shows the maximum change in temperature for undamaged, light, medium, and heavily damaged region for varying input power to the horn. Apparent is the reduced ΔT as damage increases, especially at the higher horn powers. The only exception is the most heavily damaged regions, which showed some anomalous behavior at the lower horn power settings. This may be due to the fact that in the heavy damaged region, the matrix has been excessively charred and the fibers are separated from the matrix. The reduction in the fiber matrix interface contact possibly reduces the contribution of frictional heating, leading to lower rate of increase compared to other damages. These results indicate that NCATS has significant potential in detecting heat damage in composite materials. Detailed measurements on a separate composite system have shown that the NCATS results correlated with a loss of mechanical strength [31-34].

d. Detection of cracks in an aluminum aerospace component

The previous two examples of NCATS were related to detection of plasticity in metallic materials and thermal damage in polymer matrix composites. The damage evaluation in both cases was evaluated using the conversion of acoustic energy into heat. It was hypothesized in the evaluation of accumulated damage due to tensile loading in Ti-6Al-4V, formation of internal voids and micro-cracks and the friction between the faces of the cracks produce additional heating. It has been observed that in a closed crack, the friction between the faces of the crack can generate heat that is far greater than the heat produced by direct interaction between the acoustic waves and the material. Imaging of the heat generation by the frictional heating of the cracks has been used effectively to detect cracks in materials and components [8-12]. While the experiments reported in the literature have been performed with a direct contact of the acoustic horn with the sample/structure the present example was chosen to demonstrate the potential of the NCATS technique for imaging cracks. The structure used to demonstrate this was a large 460 mm dia., 13 mm thick and 180 mm wide aluminum wheel component. A circumferential crack was identified by more traditional NDE techniques of ultrasonics and eddy current. The approximate length of the crack was 30 mm. To detect the crack in the wheel using NCATS, the wheel was supported on three metallic hemispheres. The acoustic horn was placed on the outside of the wheel approximately in the radial direction. The distance between the horn and the wheel was set to approximately 300 μm. The power of the horn was set at 1000 W and the pulse duration of 250 ms was used. The IR camera was placed above the wheel viewing the region directly opposite to the horn tip. After exciting the horn a series of thermal images as a function of time was collected. One of the images that reveal the crack is provided in Fig 10. The contrast in the image is due to the variation in the conversion of acoustic energy to heat by aluminum. The presence of crack modifies the uniform conversion of acoustic energy to heat. The variation in this heat generation helps in detecting and identifying the crack.

Although cracks can be detected and identified using NCATS, it would be necessary to scan the entire structure point by point. Alternative approaches such as Sonic IR or thermosonix use the large amplitude motion of the entire structure to generate heat in local regions where cracks are present, and being full field visualizing techniques are more convenient for such applications.

Conclusions/Summary

This paper discussed the development and initial assessment of a new non-contact acousto-thermal NDE method that interrogates the ability of a material to convert acoustic energy to heat. To better understand the basic mechanisms and the material properties involved in the process of the acousto-thermal conversion, the loss of acoustic energy into heat during the propagation of the acoustic wave in the material was analyzed. An expression that relates the change in the temperature of the material due to the propagation of an acoustic wave of frequency f and amplitude σ_{max} to the elastic (E and tan δ) and thermal (k and C_p) properties of the material has been used to establish that the conversion of acoustic energy to heat is a combination of both thermal and elastic properties of the material and forms the physical basis of the acousto-thermal NDE method. An experimental setup consisting of an ultrasonic horn capable of producing high amplitude acoustic waves, a high sensitivity IR camera, and computer data acquisition hardware were used to detect and measure the change in the temperature of various samples. The IR camera was calibrated in the room temperature range and the sensitivity (NETD) was established to be 0.0125 C per count. Since the temperature changes in the material depend on the amplitude of the acoustic waves, the distance between the acoustic horn and the sample, and the duration of the acoustic excitation, a systematic study was performed to optimize these parameters. Temperature changes in a sample of Ti-6Al-4V due to acoustic interaction was measured for varying input power, for varying distances between sample and the horn, and for varying duration of excitation to establish optimal experimental conditions. Measurement of the acoustic horn displacements at increasing power settings was used to establish a distance of 200 μm between the acoustic horn and the sample is required to prevent horn-sample contact. A detectable temperature change can be observed with a minimum horn-sample distance and maximum horn power. However, from an application stand point longer excitation time, larger horn tip sample distance, and minimum excitation power achieve the same temperature change and should be used to avoid horn-sample contact and any possibility of excitation induced damage.

Optimized experimental conditions were used to demonstrate the applicability of the NCATS technique for NDE of accumulation of plasticity in Ti-6Al-4V and thermal damage in polymer matrix composites. Feasibility of the technique to detect and image cracks was demonstrated by imaging a crack in aluminum alloy component. Further improvements for quantitative nondestructive evaluation of materials state will require additional analysis, testing, and theoretical/computational modeling of the technique.

Acknowledgements

This work was performed as a part of the on-site research in the NDE Branch, Air Force Research Laboratory, Dayton, Ohio on contract FA8650-09-D-5224 and F33615-03-C-5219. The authors thank Dr. Lindgren, and Dr. Russ, RXLP, AFRL, WPAFB, for critical reading and constructive comments on the manuscript. Authors thank Mr. Ed Klosterman and Mr. Rick Reibel for their help in the optimization of the experimental setup and measurements.

REFERENCES

1. W. T. Thomson, Quart. J. Pure & Appl. Math. **1**, 57 (1857).

2. N. Harwood and W. M. Cummings, "Thermoelastic Stress Analysis," Adam Hilger, New York (1991).

3. G. Caglioti, "The Thermo-elastic Effect: Statistical Mechanics and Thermodynamics of the Elastic Deformation," In Mechanical and Thermal Behavior of Metallic Materials, Ed. G. Caglioti and A. F. Milone, North-Holland, New York (1982).

4. R.B. Mignogna, R.E. Green, Jr., J.C. Duke, Jr., E.G. Henneke II, and K.L. Reifsnider, Ultrason. 159 (1981).

5. J. Rantala, D. Wu, and G. Busse, Res. Nondestruct. Eval. **7**, 215 (1995).

6. L.D. Favro, Xiaoyan Han, Zhong Ouyang, Gang Sun, Hua Sui, and R.L. Thomas, Rev.Sci. Instr**. 71**, 2418 (2000).

7. L. D. Favro, X. Han, L. Xiaoyan, L. Ouyang, L. Zhong, G. Sun, R. L. Thomas, A. Richards, AIP Conference Proceedings, **557**, 478 (2001).

8. X. Y. Han, L. D. Favro, R. L. Thomas, AIP Conference Proceedings, **657**, 500 (2003).

9. E. G. Henneke II, K. L. Reifsnider, and W. W. Stinchcomb, J. Metals **31**, 11 (1979).

10. K. L. Reifsnider, E. G. Henneke, W. W. Stinchcomb, "The Mechanics of Vibrothermography", in Mechanics of Nondestructive Testing, pp. 249–276, ed. W. W. Stinchcomb ,Plenum Press, New York, (1980).

11. X. Han, M. S. Islam, G. Newaz, L.D. Favro, R.L. Thomas, J. Appl. Phys, **99**, 074905 (2006).

12. X. Han, L.D. Favro, Z. Ouyang, and R.L. Thomas, J. Adhesi, **76**, 151 (2001).

13. D. Mayton, E. Lindgren, "Nondestructive Evaluation (NDE) Technology Initiatives Program (NTIP) Delivery Order 0029: Advanced Thermosonic Methods (Sonic IR)" Air Force Research Laboratory Technical Report, AFRL-ML-WP-TM-2004-4141 (2003).

14. W.O. Miller, I. M. Darnell, M.W. Burke, C. L Robbins, Thermosense XXV, Proc SPIE v. **5073**, p406-416 (2003).

15. A. Shyam, C. J. Torbet, S. K. Jha, J. M. Larsen, M. J. Caton, C. J. Szczepanski, T. M. Pollock, J. W. Jones, "Development of Ultrasonic Fatigue for Rapid, High Temperature Fatigue Studies in Turbine Engine Materials," Superalloys 2004, pp. 259-268 (2004).

16. C. Bathais, P. C. Paris, "Giga Cycle fatigue in Mechanical Practice," Marcel Dekker, New York (2005).

17. P. Bajons, K. Kromp, W. Kromp, H.Langer, B. Weiss, R. Stickler,
In: Ultrasonics international 1975; Proceedings of the Eleventh Conference, IPC Science and Technology Press, London, 1975, p. 95-101, (1975).

18. H. Roser, N. Meyndorf, S. Sathish, and T. E. Matikas, in "Nondestructive Methods for Materials Characterization," Ed. G. Y. Baaklini, N. Meyndorf, T. E. Matikas, R. S. Gilmore, Materials Research Society, Symposium Proceedings Vol. 591, pp. 73-78, MRS, Warrendale, (2000).

19. N. G. H. Meyendorf, H. Rosner, V. Kramb, S. Sathish, Ultrason. **40**, 427 (2002).

20. S. Suresh, "Fatigue of Materials," Cambridge University Press, New York (2002).

21. W. Grafe, "Time-dependant Mechanical Properties of Solids," Trans. Tech. Pub., Enfield, NH (2008).

22. A. S. Nowick and B. S. Berry, "Anelastic Relaxation in Crystalline solids,", Academic Press, New York (1972).

23. Y. Li, D. Pan, C. Yang, Y. Luo, "NETD test of high-sensitivity infrared camera," Proceedings of the SPIE, V. 6723, 67233(2007).
3rd International Symposium on Advanced Optical Manufacturing and Testing Technologies: Optical Test and Measurement Technology and Equipment. Edited by Pan, Junhua; Wyant, James C.; Wang, Hexin.

24. Y. Zhao, J. Choi, R. Horowitz, A. Majumdar, J. Kitching, P. Norton, "Characterization and Performance of Optomechanical Uncooled Infrared Imaging System" Infrared Technology and Applications XXVIII, pp. 164-170, Ed. F. B. Andresen, G. F. Fulop, Marija Strojnik, Proceedings of SPIE Vol. 4820 (2003)

25. W.J. Parker, R.J. Jenkins, C.P. Butler, G.L. Abbot, J. Appl. Phys., **32**, 1679 (1964).

26. X. P. Maldague, “Theory and Practice of Infrared Technology for Nondestructive Testing, NY : John Wiley & Sons, 200.

27. Nondestructive Handbook, Infrared and Thermal Testing, Volume 3, X. Maldague technical ed., P. O. Moore ed., 3rd edition, Columbus, Ohio, ASNT Press, 2001, 718 p

28. S. Shepard, Mater. Evalu. **57**, 460 (2006).

28. J. L. S. Maurer, “Characterization of Accumulated Fatigue Damage in Ti-6Al-4V Plate Materials Using Transmission Electron Microscopy and Nonlinear Acoustics,” Dissertation, University of Dayton, Dayton, OH (2001).

29. R.K. Nalla, B.L. Boyce, J.P. Campbell, J.O. Peters, R.O. Ritchie, Met and Mat Trans A, **33A**, 899 (2002).

30. J.T. Welter, G. Mallott, N. Schehl, S. Sathish, K. V. Jata and M. P. Blodgett, AIP Conf. Proc, **v.1211**, 1397 (2010).

31. H. McShanem R. Cramer, K. Miller, T. Stephens, M. Nadler, R. Yee, 42nd International SAMPE Symposium Proc., 890 (1997)

32. J. Welter, S. Sathish, S. Ripberger, E. Lindgren, AIP Conf. Proc., **v.892**, 1052 (2007).

33. S. Sathish, J. T. Welter, R. Reibel and C. Buynak, AIP Conf. Proc, **v.820**, 1015 (2006)

34. J. Welter, S. Sathish, S. Ripberger, E. Lindgren, Mater. Eval., **65**, 823 (2007).

FIGURE CAPTIONS

Figure1. Schematic of the NCATS experimental setup.

Figure 2: Displacement amplitude across the ultrasonic horn during vibration. (Maximum displacement: 180 μm)

Figure3. Displacement of the horn with increasing input power.

Figure 4: Figure 4: NCATS Time –Temperature signatures at different input powers to the horn. Distance between horn and sample: 300 μm. Duration of excitation: 250 ms. Sample: Ti-6Al-4V.

Figure 5: NCATS Time –Temperature signatures for increasing excitation time of the horn. Input Power to the horn 1000W. Distance between sample and horn: 200 μm. Sample: Ti-6Al-4V.

Figure 6: Change in maximum temperature in the sample for varying distances between sample and the horn. Horn power settings: 1000 W and 800 W. Duration of excitation: 250 ms. Sample: Ti-6Al-4V

Figure 7: Maximum change in temperature with increasing plastic strain in Ti-6Al-4V.

Figure 8: Composite Strain-Strain curve for Ti-6Al-4V sample.

Figure 9: Maximum temperature in NCATS measurements on heat damaged composite samples with increasing power to the horn.

Figure 10: NCATS imaging of a crack in aluminum wheel component.

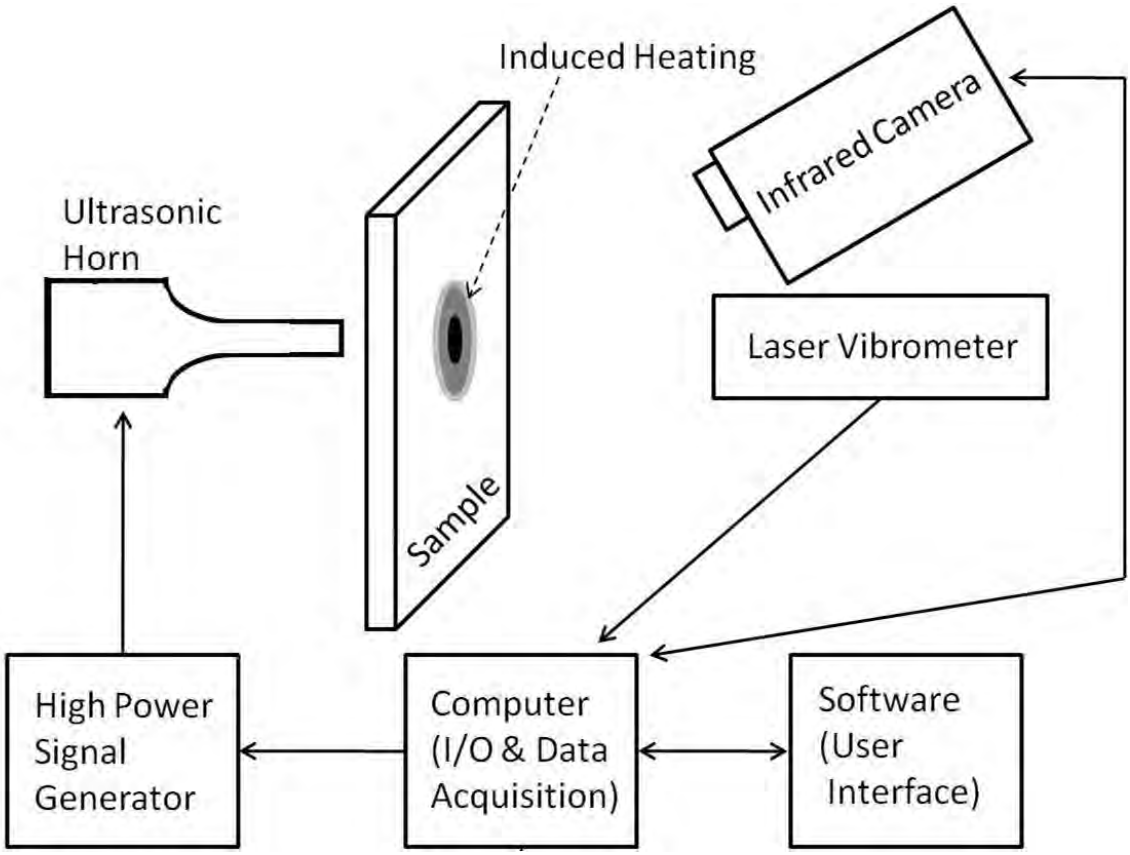

Figure1. Schematic of the NCATS experimental setup.

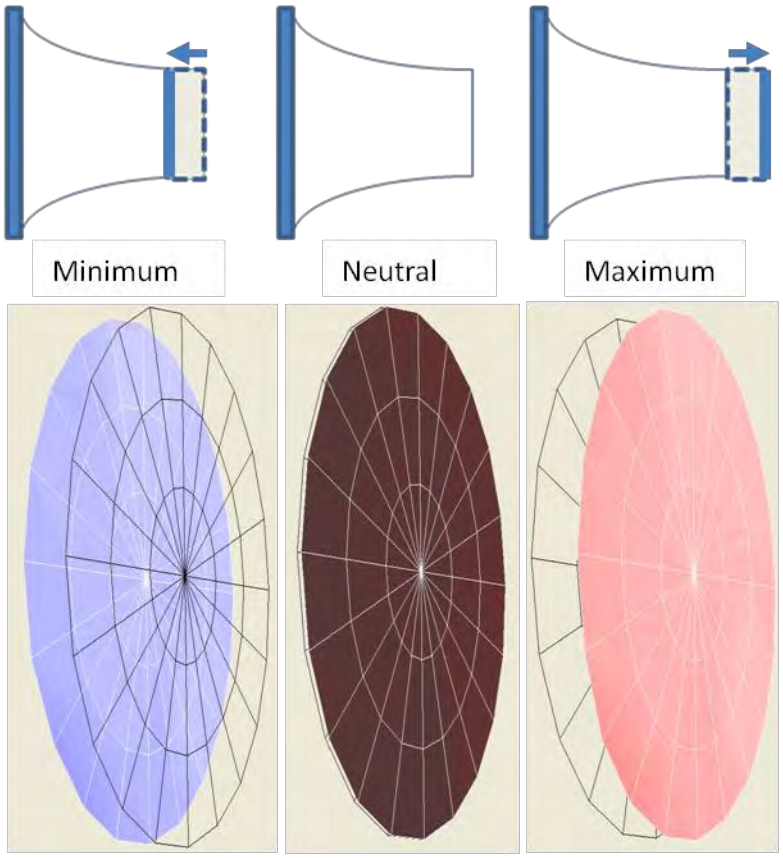

Figure 2: Displacement amplitude across the ultrasonic horn during vibration. (Maximum displacement: 180 μm)

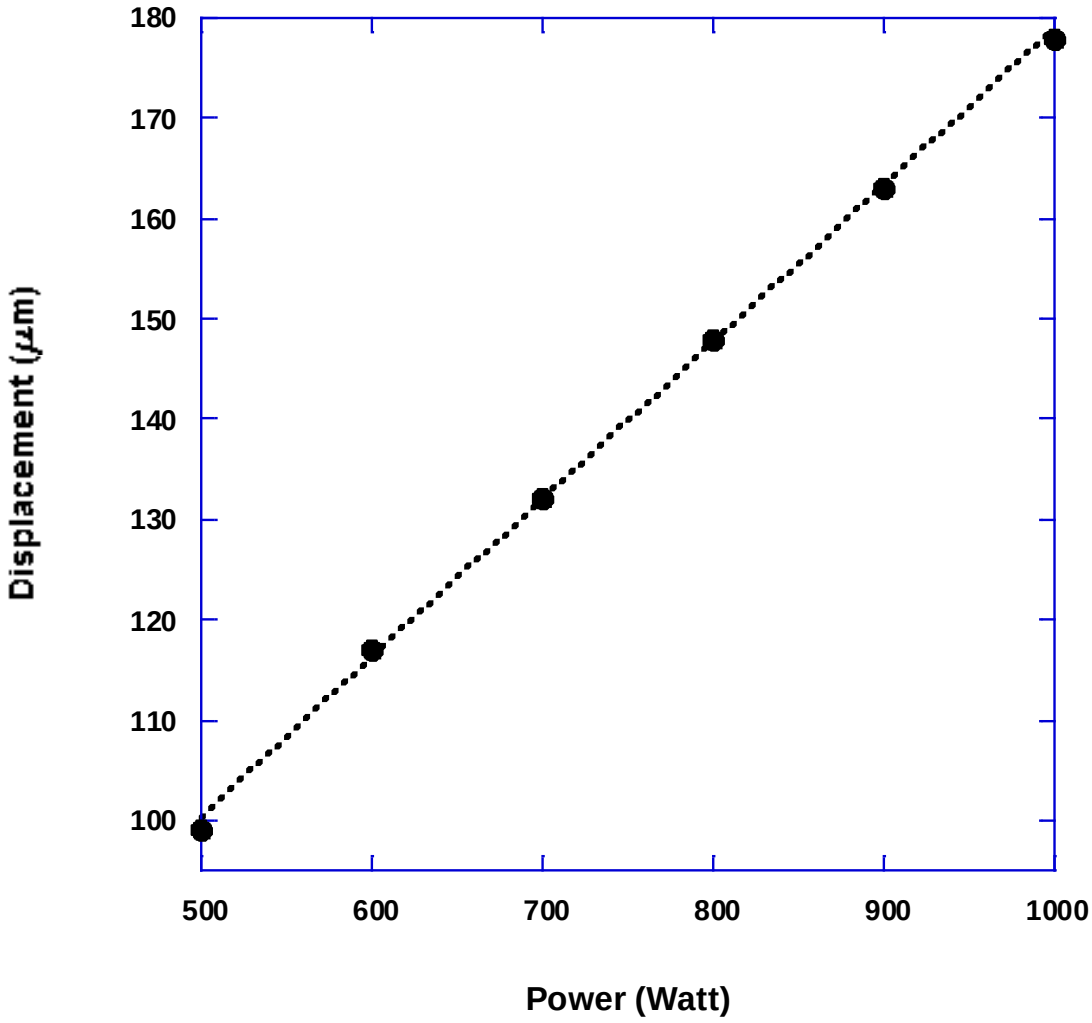

Figure 3. Displacement of the horn with increasing input power.

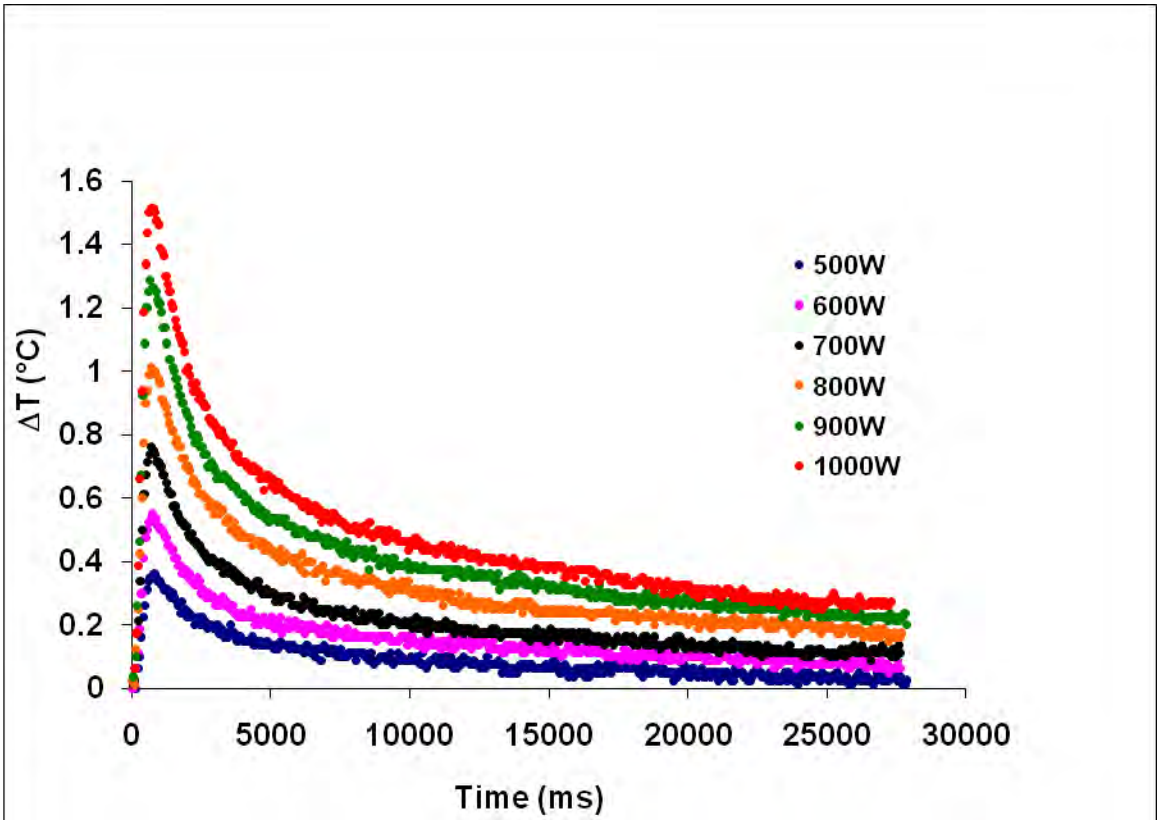

Figure 4: NCATS Time –Temperature signatures at different input powers to the horn.

Distance between horn and sample: 300 μm. Duration of excitation: 250 ms.

Sample: Ti-6Al-4V.

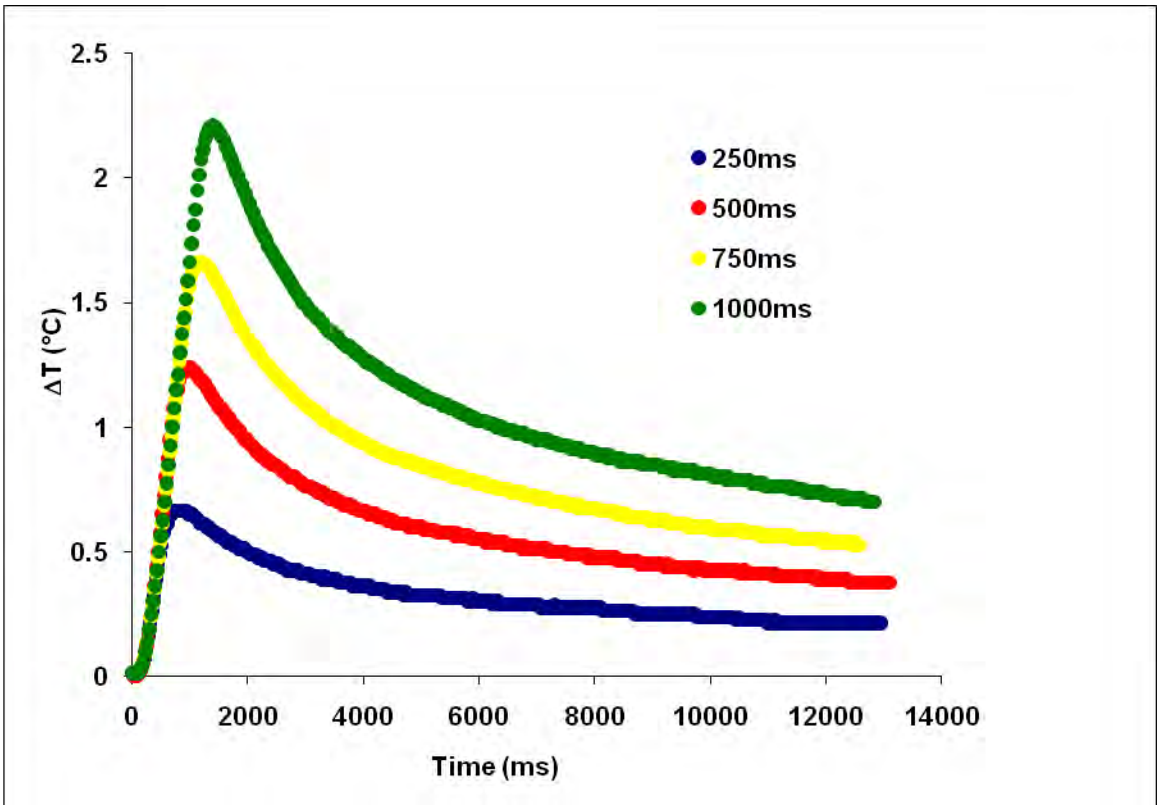

Figure 5: NCATS Time –Temperature signatures for increasing excitation time of the horn. Input Power to the horn 1000W. Distance between sample and horn: 200 μm. Sample: Ti-6Al-4V.

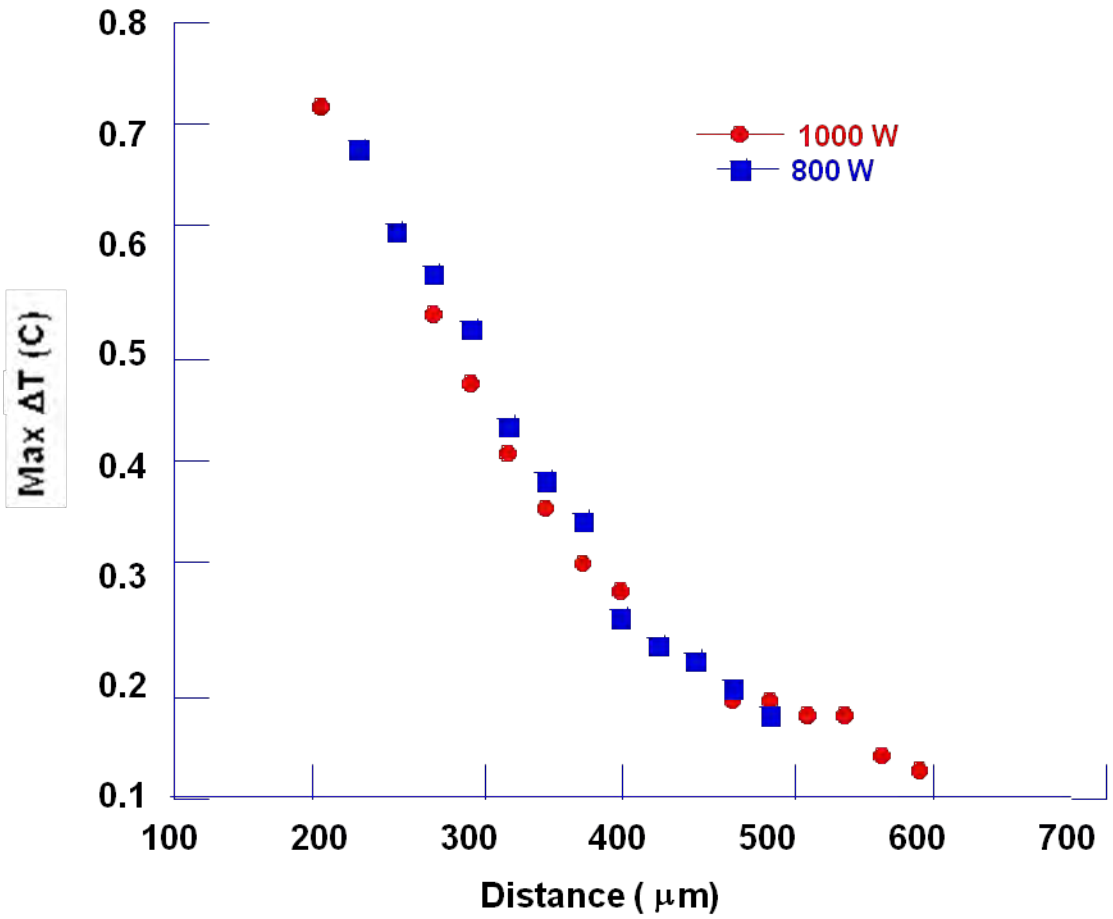

Figure 6: Change in maximum temperature in the sample for varying distances between sample and the horn. Horn power settings: 1000 W and 800 W. Duration of excitation: 250 ms. Sample: Ti-6Al-4V

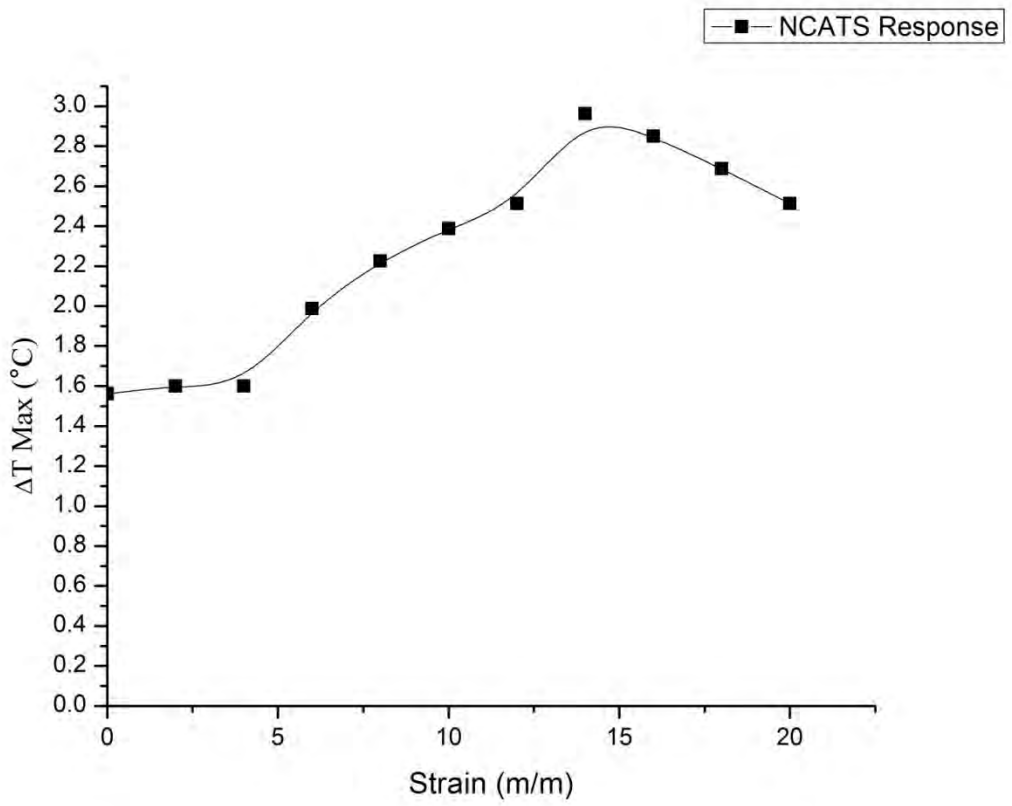

Figure 7: Maximum change in temperature with increasing plastic strain in Ti-6Al-4V.

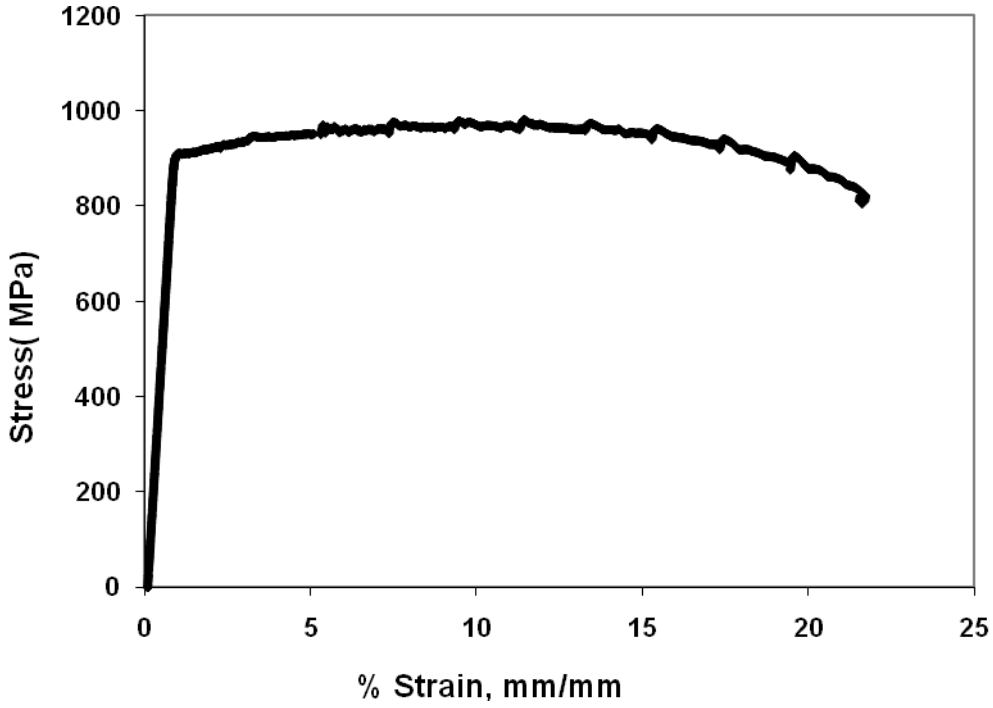

Figure 8: Composite Strain-Strain curve for Ti-6Al-4V sample.

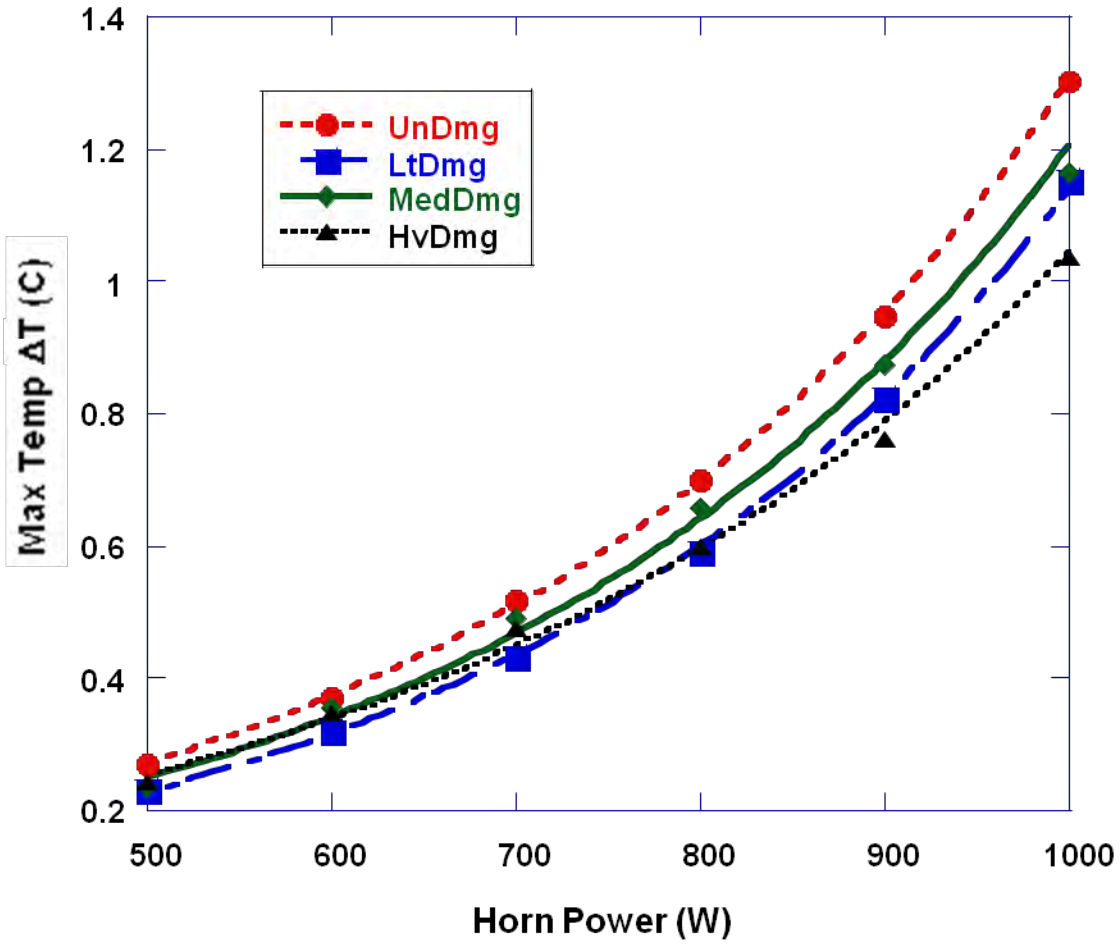

Figure 9: Maximum temperature in NCATS measurements on heat damaged composite samples with increasing power to the horn.

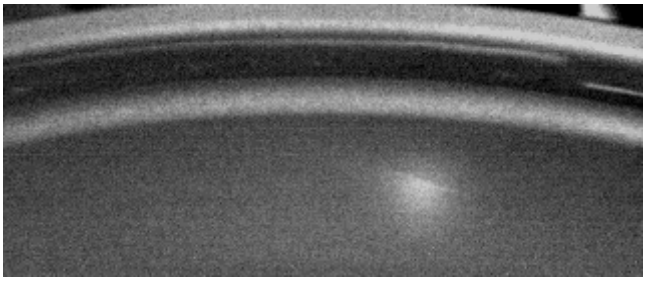

Figure 10: NCATS imaging of a crack in aluminum wheel component.